



Received August 2001
 Revised November 2001
 Accepted November 2001

Fire and smoke distribution in a two-room compartment structure

G.H. Yeoh

*Australian Nuclear Science and Technology Organisation (ANSTO),
 PMB 1, Menai, NSW 2234, Australia*

R.K.K. Yuen, E.W.M. Lee and S.C.P. Chueng

*Department of Building and Construction, City University of Hong Kong,
 Tat Chee Avenue, Kowloon, Hong Kong*

Keywords Computational fluid dynamics, Turbulence, Combustion, Radiation

Abstract This paper presents a comparison of numerical predictions employing a Computational Fluid Dynamics fire model against a series of turbulent buoyant fire experiments recently carried out in a two-room compartment structure by Nielsen and Fleischmann at the University of Canterbury, New Zealand. The model incorporates turbulence, combustion, soot generation and radiation due to a fire. An evaluation of the various approaches—volumetric heat source approach or a more sophisticated handling the fire through a combustion model—is carried out. The effect of radiation due to combustion products and soot is also investigated. The model considering combustion with radiation contribution by both the combustion products and soot provides the best agreement between the predicted results and measured data. The presence of soot is seen to significantly augment the global radiation process within the two-compartment enclosure.

Nomenclature

$C_\alpha, C_\beta, C_\gamma$	= soot pre-exponential constants	\tilde{U}	= Favre-averaged velocity vector
C_r	= eddy-break up constant	U_{th}	= thermophoretic velocity
E_b	= blackbody radiation	\tilde{X}	= Favre-averaged mole fraction
f_v	= soot volume fraction	<i>Greek symbols</i>	
I_j	= radiation intensities	$\bar{\alpha}$	= rate of particulate number density nucleation
k_a	= gas radiative absorption coefficient	$\bar{\beta}$	= rate of coagulation of soot
\tilde{m}	= Favre-averaged mass fraction	$\bar{\delta}$	= rate of soot volume fraction nucleation
n	= particulate number density	$\bar{\gamma}$	= rate of surface growth of soot
N_0	= Avogadro's number	$\bar{\rho}$	= mean density
R	= reaction rate	ε	= dissipation rate of turbulent energy
s	= stoichiometric oxygen-to-fuel mass ratio		
T_α, T_γ	= soot activation temperatures		
\bar{T}	= mean temperature		



κ	= turbulent kinetic energy	<i>Subscripts</i>	
ρ_s	= soot density	fu	= fuel
μ	= molecular viscosity	ox	= oxygen
μ_t	= turbulent viscosity	n	= particulate number density
ν	= kinematic viscosity	Pr	= Prandtl number
σ_i	= Prandtl/Schmidt number	s	= soot
σ	= Stefan-Boltzman constant	Sc	= Schmidt number
ξ_j, η_j, ζ_j	= direction cosines		

1. Introduction

As building codes, regulations and standards move from the usual prescriptive-based to more performance-based, fire engineers are given the freedom to employ innovative design, with the aim of more efficient use of space, building materials, and a more cost effective design, to solve fire-related problems. With the ever rapid advancement of computer processing power and reducing computational times, the option to use computational fluid dynamics (CFD) techniques is becoming viable for fire engineers to simulate enclosure fires to determine and evaluate the performance and safety levels in buildings.

The CFD evaluation of smoke movement has changed comparatively little from the earliest computations such as JASMINE (Markatos *et al.*, 1982), PHOENICS (Yang, 1994) and FLOW3D (Beard, 1997). All these models have so far adopted a simplified approach in representing the fire as spatially distributed heat sources—the volumetric heat source approach.

Comparison of CFD models, incorporating combustion and radiative exchange, by Lewis *et al.* (1997) demonstrated the importance that such representations can have on the flow field development. They also showed that the volumetric heat source approach failed to reproduce the two-layer structure prevalent in enclosure fires as seen through Steckler *et al.* (1984) room fire experiments. For an accurate heat transfer and fluid flow predictions, the inclusion of combustion and radiation models are indispensable.

Another fundamental standpoint, the treatment of radiative heat transfer, critical to flame spread modelling, is compromised in the absence of a satisfactory description of the spatially varying absorption coefficient of which soot is a major contributor. Without some representation of finite rate chemistry in the fuel-rich pyrolysis regions within the fire, it is not possible then to predict particulate carbon emission levels from the fire source. Wen *et al.* (2001) demonstrated in their analysis of fire in a large compartment space that soot radiation has a significant impact on the flow and thermal characteristics.

With the increasing complexity introduced in the CFD models, the inclusion of turbulence, combustion, radiation and soot sub-models, concern for the accuracy for building fire simulation becomes important. In order to establish confidence in the usage of these models in fire safety studies, they can only be useful if they are validated.

The objectives of this paper are:

- It is imperative that the use and validation of the CFD model extends beyond the single compartment geometry in order that it can be of use for complex geometries. We therefore extend and verify our CFD model (Yuen *et al.*, 2001, Yeoh *et al.*, 2001), recently validated against “Steckler” single compartment problem, against a series of two-room compartment fire experiments of turbulent buoyant diffusion flames recently performed by Nielsen and Fleischmann (2000) at the University of Canterbury, New Zealand;
- We will demonstrate the applicability of the volumetric heat source approach and the need to include a combustion model to resolve the fire chemistry; and
- We will investigate the radiation contribution by the gaseous combustion products, carbon dioxide (CO₂) and water vapour (H₂O), and soot affecting the global radiation within the compartment.

2. Mathematical model

The fluid flow and heat transfer within the two-compartment structure are described by a three-dimensional *Favre*-averaged transport equations for mass, momentum and energy. The eddy-viscosity concept is employed for the representation of the turbulent diffusivities in the governing equations due to turbulence. This is expressed by the solution of the standard κ - ϵ turbulent model with additional source terms to account for buoyancy effects.

2.1 Combustion modelling

In an eddy break-up (EBU) model by Magnussen and Hjertager (1976), an explicit equation for the mass fraction of fuel is solved:

$$\frac{\partial \tilde{m}_{fu}}{\partial t} + \nabla(\bar{\rho} \tilde{U} \tilde{m}_{fu}) - \nabla \left[\left(\frac{\mu}{\sigma_{fu,Sc}} + \frac{\mu_t}{\sigma_{fu,Pr}} \right) \nabla \tilde{m}_{fu} \right] = -R_{fu} \quad (1)$$

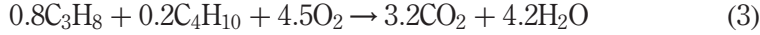
The EBU model assumes that the chemistry is fast and therefore only the turbulent mixing is rate controlling. The mass rate of fuel consumption may be written as

$$R_{fu} = C_r \bar{\rho} \frac{\epsilon}{\kappa} \min[\tilde{m}_{fu}, \tilde{m}_{ox}/s] \quad (2)$$

where $\bar{\rho}$ is the time-averaged density; \tilde{m}_{fu} and \tilde{m}_{ox} are the *Favre*-averaged mass fractions of fuel and oxidant, respectively; s denotes the stoichiometric oxygen-to-fuel mass ratio; $\min[]$ denotes the minimum of the comparison arguments; C_r is an empirical constant usually taken as 4.

LPG (Liquefied Petroleum Gas) as described in Nielsen and Fleischmann (2000) comprises of approximately 80% of propane (C₃H₈) and 20% of butane

(C₄H₁₀). The global, one-step description of LPG combustion is assumed and can be written as:



Fire and smoke
distribution in a
compartment

2.2 Soot modelling

Unlike the concentrations of the major species in diffusion flames which result from chemistry fast compared with mixing and therefore exhibiting an important measure of invariance, soot mechanisms are comparatively slow and has a pronounced additional dependence on temperature history. The kinetic theory of soot formation proposed by Tesner *et al.* (1971) has been employed by many. Whilst this model has been applied to room fire simulations (Luo and Beck, 1996, for example) its focus solely on particle number density neglects the important role of surface growth in relation to soot mass addition, and does not then incorporate any particle size evolution. Without knowledge of particle size, the aerosol surface area cannot be determined and heterogeneous chemical process like oxidation cannot be satisfactorily determined.

The recently proposed soot model that incorporates the essential physical processes of soot nucleation, coagulation and surface growth developed principally by Moss *et al.* (1988) is of particular interest. This semi-empirical soot model is attractive since soot production is described simply in terms of local temperature and mole fraction of fuel. The representation of soot properties involves just two variables—soot volume fraction, f_v , and the particulate number density, n .

The *Favre*-averaged transport equations for the soot particulate number density and soot volume fraction can be written as

$$\frac{\partial(\bar{\rho}\tilde{\zeta}_n)}{\partial t} + \nabla(\bar{\rho}\tilde{U}\tilde{\zeta}_n) + \nabla(\bar{\rho}U_{\text{th}}\tilde{\zeta}_n) - \nabla\left[\left(\frac{\mu_t}{\sigma_{n,Pr}}\right)\nabla\tilde{\zeta}_n\right] = \bar{\alpha} - \bar{\rho}^2\bar{\beta}\tilde{\zeta}_n^2 \quad (4)$$

$$\frac{\partial(\bar{\rho}\tilde{\zeta}_s)}{\partial t} + \nabla(\bar{\rho}\tilde{U}\tilde{\zeta}_s) + \nabla(\bar{\rho}U_{\text{th}}\tilde{\zeta}_s) - \nabla\left[\left(\frac{\mu_t}{\sigma_{s,Pr}}\right)\nabla\tilde{\zeta}_s\right] = \bar{\delta} - N_0^{1/3}\bar{\rho}\bar{\gamma}\tilde{\zeta}_s^{2/3}\tilde{\zeta}_n^{1/3} \quad (5)$$

where the tilde denotes a *Favre* average and where $\zeta_n = n/\rho N_0$ and $\zeta_s = \rho_s/\rho f_v$. The particulate number density is represented by n . N_0 is the Avogadro's number (6.0223×10^{26}) and ρ_s is the soot density. U_{th} is the mean thermophoretic velocity component that can be expressed by $U_{\text{th}} = -0.54\nu\nabla(\ln\bar{T})$ where ν is the kinematic viscosity. The rate of particle nucleation is given by $\bar{\alpha} = C_\alpha\bar{\rho}^2\bar{T}^{1/2}\bar{X}_{\text{fu}}\exp(-T_a/\bar{T}) = \bar{\delta}/144$ where \bar{T} is the mean temperature. The coagulation of soot is described by Smoluchowski (Fuchs, 1964) expression: $\bar{\beta} = C_\beta\bar{T}^{1/2}$. The last term in equation (5) represents the surface growth of soot suggested by Syed *et al.* (1990) which contained a

linear dependence on aerosol surface area, and is controlled by the rate relationship: $\bar{\gamma} = C_\gamma \bar{\rho} \bar{T}^{1/2} \bar{X}_{fu} \exp(-T_\gamma/\bar{T})$.

From a detailed chemical kinetic models of fuel pyrolysis it is possible to identify specific hydrocarbon species that are precursors to drive the nucleation and surface growth expressions through the mole fraction \bar{X}_{fu} . Lindstedt (1994) suggested acetylene (C_2H_2). Nevertheless, detailed reaction mechanisms, and hence distributions of minor species concentrations are not accessible for the fuel LPG hence a simpler strategy is then necessary. In this study, we have used the parent fuel LPG as the precursor for soot formation similar to Syed *et al.* (1990) that have used methane. As LPG contains components of fuels that are predominantly weakly sooting flames, and since no pre-exponential constants C_α , C_β and C_γ and activation temperatures T_α and T_β are available for LPG, as a first step, we adopt values that have been pre-determined for methane combustion. The values used in the calculations are

$$\begin{aligned} C_\alpha &= 65\,400 \text{ m}^3/\text{kg}^2 \text{ K}^{1/2} \text{ s} \\ C_\beta &= 1.3 \times 10^7 \text{ m}^3/\text{K}^{1/2} \text{ s} \\ C_\gamma &= 0.1 \text{ m}^3/\text{kg}^{2/3} \text{ K}^{1/2} \text{ s} \\ T_\alpha &= 46\,100 \text{ K} \\ T_\gamma &= 12\,600 \text{ K} \end{aligned}$$

2.3 Radiation modelling

Global radiation in fires represents an essential part of fire modelling because of the radiative exchange between the gaseous and soot elements and the compartment boundaries. The discrete ordinates method (DOM), an efficient and relatively accurate method for calculating radiative transfer, has been incorporated in these calculations. The scattering coefficients for fine dispersed soot particles ($\sim 0.1 \mu\text{m}$) are considered to be negligible compared to the respective absorption coefficients (Luo *et al.*, 1997). The radiative transfer equation, ignoring any scattering effects, can be written as

$$\xi_j \frac{\partial I_j}{\partial x} + \eta_j \frac{\partial I_j}{\partial y} + \zeta_j \frac{\partial I_j}{\partial z} = -k_a I_j + k_a E_b \quad (6)$$

The blackbody radiation is defined as $E_b = \sigma \bar{T}^4$. The direction cosines ξ_j , η_j and ζ_j represent a set of directions for each of the radiation intensities I_j which span over the total solid angle range of 4π around a point in space. The integrals over solid angles are approximated using the S_4 numerical quadrature (Jamaluddin and Smith, 1988).

The mean absorption concept of Hubbard and Tien (1978) are used to calculate the absorption coefficients of the gaseous. In this approach, the Elsasser narrow-band model is used for the absorbing gases. For the evaluation

of the contribution of CO_2 to the mean Planck mean absorption coefficient, the vibration-rotation bands considered are at 15, 10.4, 9.4, 4.3, 2.7 and 20 μm . For H_2O , the 20 μm pure rotation and the 6.3, 2.7, 1.9 and 1.4 μm vibration-rotation bands are included. For soot, the absorption coefficient is based on an expression from Kent and Honnery (1990).

3. Numerical procedure

The conservation equations are discretised using the finite volume method. A Hybrid differencing scheme is employed for the convection terms. The velocity and pressure linkage is achieved through the SIMPLE algorithm. The discretised equations are solved using an extended three-dimensional solver of the original two-dimensional Stone's implicit procedure (Stone, 1968).

Figure 1 shows the grid distribution of the two-compartment geometry. Experimental observations by Nielsen and Fleischmann (2000) for the central fire in the burn room revealed that this configuration was symmetrical about the vertical plane bisecting the burner, doorway and open end. Mesh generation was therefore carried out on half of the room, improving the resolution of the flow and thermal fields. Numerical experiments revealed that the inclusion of an extended region away from the open end was important to correctly model the flow through the open end (Yuen *et al.*, 2001). An extended region of $3.6\text{ m} \times 4.8\text{ m}$ in plan and 6.5 m in height is attached to the two-compartment structure to isolate the end effects of the extended boundaries from the open

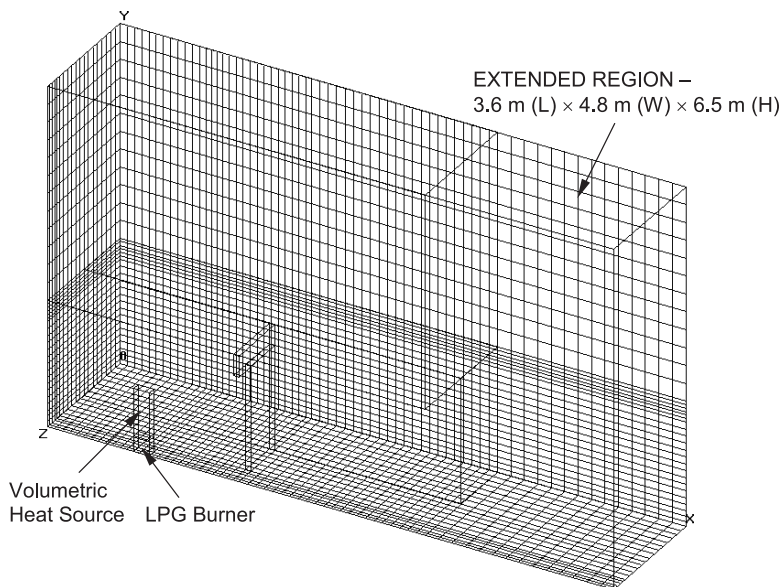


Figure 1.
Mesh distribution of the
two-compartment
geometry

end of the geometry. The computational grid is $64 \times 34 \times 19$ (i.e. a total of 41344 control volumes).

3.1 Boundary conditions

At the burner surface, the normal velocity is evaluated from the fuel burn rate. Turbulence level is assumed to be weak, so that the laminar assumption is used at this boundary. Temperature is set to be constant based on the temperature of the unburnt fuel flowing through the burner. The mass fraction of fuel is set at unity.

The condition of no-slip is imposed at the inert solid surfaces by setting all velocities to zero. The normal gradients of the mass fraction of participating species, particulate normal density and soot volume fraction are set to zero at these boundaries due to impermeability of the walls. In order to resolve the momentum and heat fluxes near the wall region, conventional logarithmic wall function was applied. Adiabatic condition is imposed for the calculation of the wall temperatures. Correspondingly, the enthalpy equation is determined from the given wall temperature when solving the energy conservation equation.

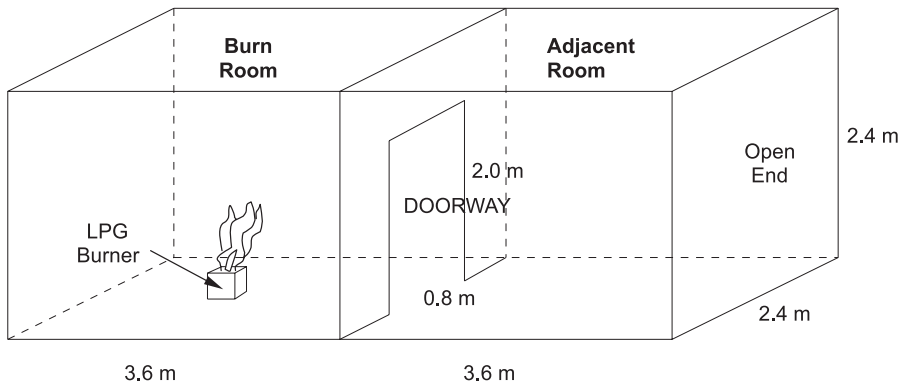
At the extended boundaries, the solution domain is treated as entraining surface on which the ambient pressure is set to be constant. The normal gradients of all dependent variables are set to zero for in-flow or out-flow conditions except for the temperature, mass fraction of participating species, particulate normal density and soot volume fraction where ambient variables are specified at this plane when the flow enters the compartment.

4. Experimental setup and instrumentation

A brief description of the experimental configuration used in the numerical calculations is described herein. More detailed information regarding the setup can be referred in Nielsen and Fleischmann (2000). Figure 2 shows the layout of the two-compartment structure. The geometry was insulated with Gib[®] Fyreline and Intermediate Service Board to minimise heat transfer and damage to the structure and instrumentation. A square sand-box LPG burner of 0.3 m wide and elevated 0.3 m above the floor was centrally located in the burn room as shown in Figure 2. Simulations carried out for comparisons against numerical and experimental results were performed for a fire size of 110 kW. During the experiments, the combustible gas flowing out of the burner was ensured to be below Froude number of unity in order to simulate buoyancy driven flames (McCaffery, 1995).

To enable the validation of vertical temperature profiles for CFD models in this study, aspirated thermocouples were placed evenly throughout the compartment. Figure 3 shows the spatially distributed thermocouple tress within the burn and adjacent rooms.

Figure 2.
Schematic drawing of the
two-compartment
structure



5. Results and discussion

Detail investigations are carried out in this study to evaluate the fire model employing the volumetric heat source approach and solving the combustion coupled with radiation and generation of soot.

The simpler strategy of employing the volumetric heat source approach to fire problems usually involves specifying a fixed volume above the fire source to represent the flaming fire. In this study, a volume size of $0.9 \times 0.3 \times 0.3 \text{ m}^3$ is taken. The volumetric heat capacity of $(110 \text{ W}/0.081 \text{ m}^3)$ is then used as an input parameter that is fed into the source term of the energy equation for fire simulation. As distribution of combustion products and soot are not accessible, a constant absorption coefficient is used in the radiation calculations. A value of 5.97 recommended by Hubbard and Tien (1978) has been used to account for the radiation loss due to combustion products.

Comparison of model predictions is carried out against series of spatial temperature measurements obtained from Nielsen and Fleischmann (2000) for a steady-state fire at 45 min. Figure 4(a)–(e) show the predicted temperature profiles against measurements from thermocouple trees located at positions “1”, “3”, “5”, “7” and “9” (see Figure 3). These thermocouple readings were





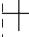
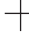
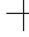


BURN ROOM					ADJACENT ROOM			
Tree 1	Tree 2	Tree 3	Tree 4	Tree 5	Tree 6	Tree 7	Tree 8	Tree 9
								
0.15 m	0.9 m	1.8 m	2.7 m	3.6 m	4.5 m	5.4 m	6.3 m	7.2 m

Figure 3.
Distribution of
thermocouple tree
positions (Crosses
indicate field trees)

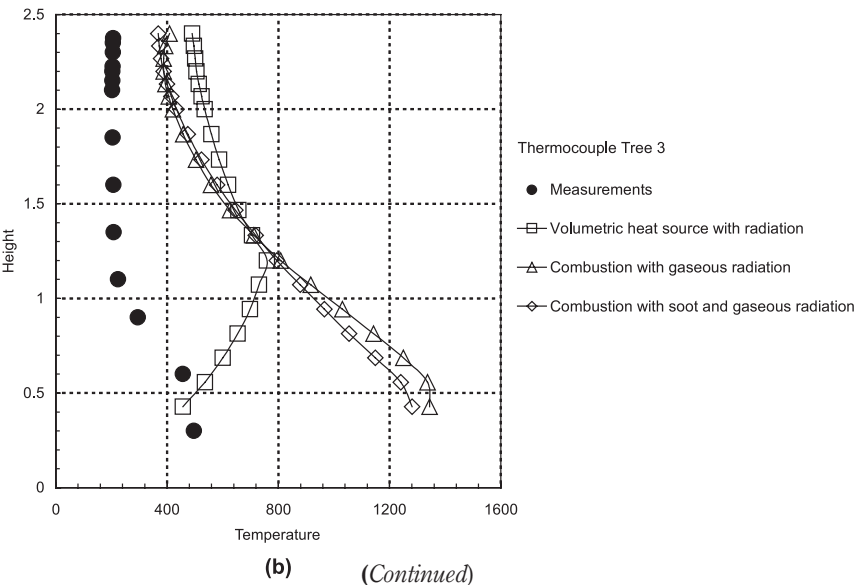
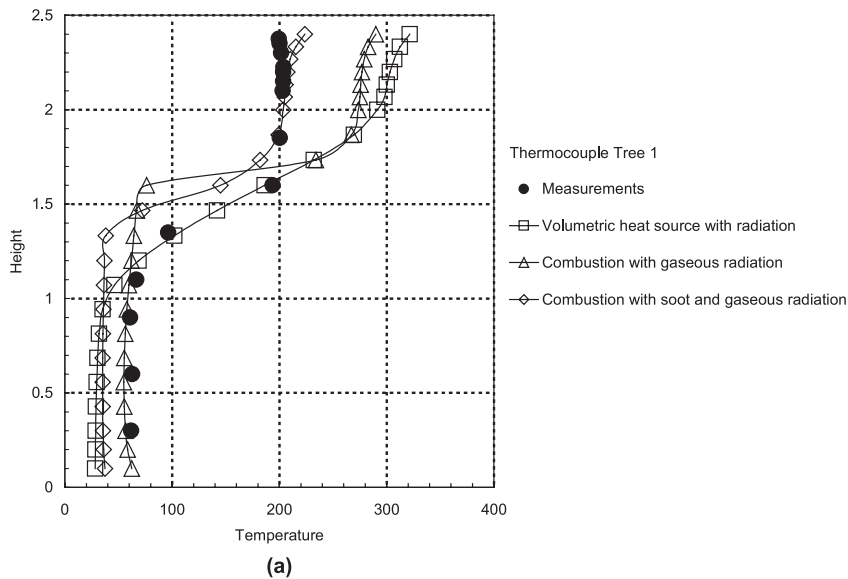


Figure 4.
 Temperature profiles (°C)
 for thermocouple trees:
 (a) Tree “1”, (b) Tree “3”,
 (c) Tree “5”, (d) Tree “7”
 and (e) Tree “9”

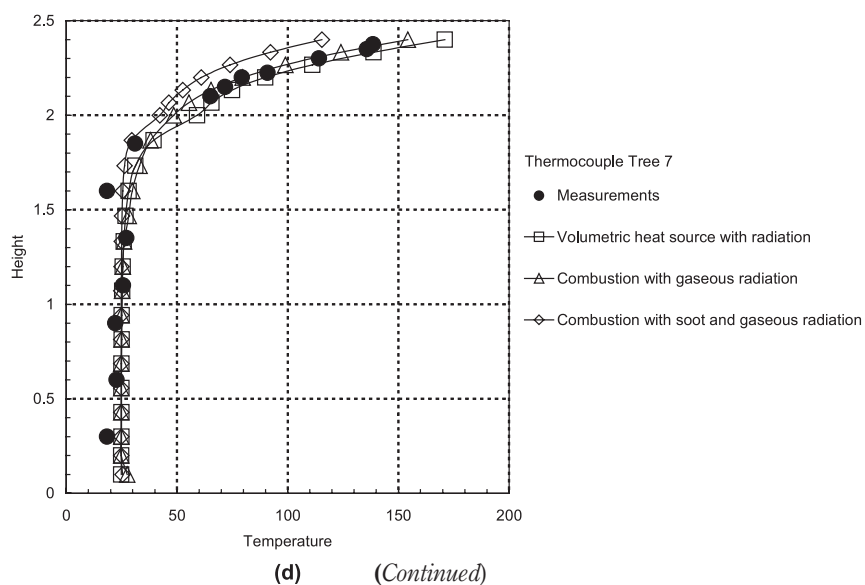
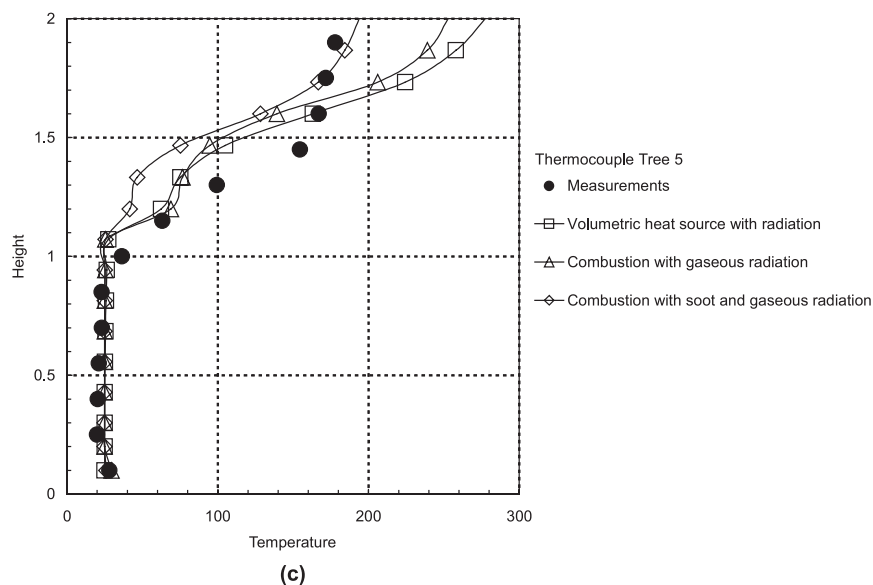


Figure 4.

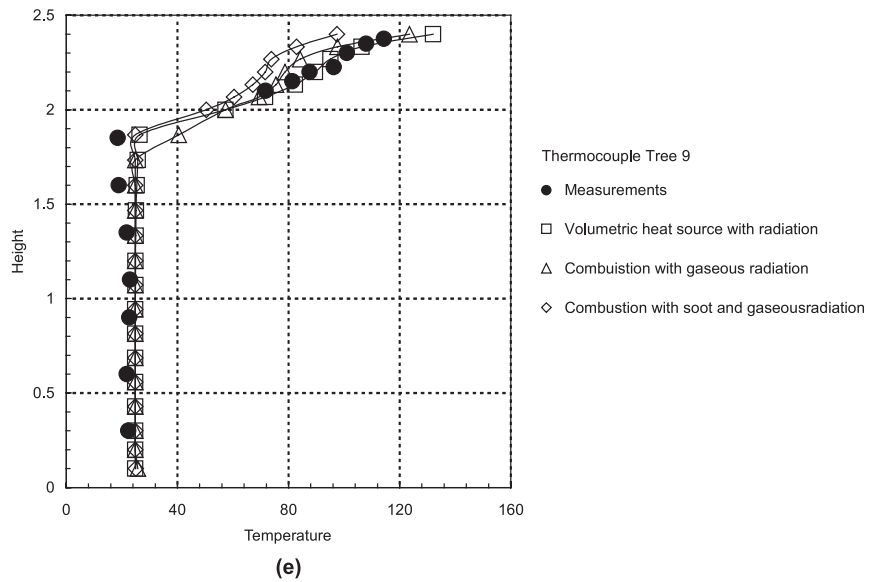


Figure 4.

selected to sufficiently represent the overall thermal response of the fire behaviour within the two-compartment structure. Position “1” reflected the thermal distribution near the end wall of the compartment. Positions “3” and “5” described the temperature distributions above the fire source and the doorway connecting both the burn and adjoining rooms. Position “9” measured the influence of the entrainment of the surrounding ambient air into the compartment while position “7” recorded the thermal interaction between the outflow temperature from the burn room and the incoming ambient air temperature in the adjoining room.

In Figure 4(b), measured temperatures were much lower than expected and not consistent with typical temperatures within the flaming fire observed in Drysdale (1986) where they should be at least 800°C. There are two reasons for lower than expected of the measured temperatures. The first is contribution due to radiation. The thermocouples in the fire area are usually very hot, and since they were not shielded, they will therefore emit radiation and will reduce the temperature of the thermocouples. The second is that the thermocouples located in the upper part of the flame will be measuring the intermittent flame temperature. This is probably a result of the unburnt LPG lowering the temperature of the thermocouple. Wen *et al.* (2001) investigated this problem and also discovered that they were inherent errors in the raw thermocouple readings due to radiation. When they corrected their experimental data, the differences between the uncorrected and corrected results due to radiation were found to be greater than 100 K.

Gross misrepresentation of the temperature behaviour above the fire source is clearly evidenced by the use of the volumetric heat source approach. Significant improvement to the temperature prediction was achieved by the consideration of combustion in the model. The inclusion of soot in the simulations was seen to only marginally affect the temperatures in comparison to the case where only gaseous radiation was considered.

Away from the fire source in the burn room, soot radiation was seen to have a more significant effect on the temperatures in comparison to its contribution within the fire plume area as illustrated by model predictions made for near the end wall (Tree 1) and doorway (Tree 5) distributions. Although steps have been taken in experiments to carefully insulate the two-compartment structure, a small degree of thermal linkage through the ceiling wall at Tree 1 position could still be observed. Present models employing adiabatic condition showed, however, temperature profiles near the ceiling pointing away from the end wall. It is noted that consideration of heat losses through the compartment walls will only affect the temperature distributions near the wall region. Hence, further refinement of the models will only serve to improve the current temperature predictions.

One distinct feature commonly found in compartment fires is the existence of a two-layer structure. At the top, the hot layer contains the hot combustion products and pollutant like soot and at the bottom, the cold layer contains the distribution of cold air entraining into the compartment. The presence of soot in the hot layer below the ceiling was seen to lower the temperatures considerably in comparison to the case of radiation contribution only from the hot combustion products. Interestingly enough or somewhat fortuitous that predicted temperatures by the volumetric heat source approach with radiation was comparable to the case considering combustion with gaseous radiation. It was only by sheer chance that the absorption coefficient chosen for the volumetric heat source approach was compatible to those of Hubbard and Tien's. In most cases, the knowledge of an appropriate value for the absorption coefficient may not be known *a priori*. Furthermore, the absorption coefficients are not constant throughout the compartment space. Such approach towards fire modelling should be exercised with caution in resolving the radiation contribution in enclosure fires.

In the adjacent room, the post-flame region, predictions made by all the different models for temperature distributions for Trees 7 and 9 showed good agreement with experimental data. Predicted temperatures whether employing just the volumetric heat source or combustion with or without soot and gaseous radiation were consistent with measured profiles. Especially a clear representation of the acute straightening of the temperatures below the 2 m height was observed comparing the measured data in Tree 9. In the adjoining room, it could be inferred that the presence of soot was only confined to the burn room. At first glance, the volumetric heat source approach could be viewed to

adequately resolve the fire dynamics within the two-compartment enclosure, judging from the good temperature predictions in the adjoining room. However, it has been demonstrated in Figure 4(b) that the model accuracy was left wanting, exposing limitations in its usage. Furthermore, the flow can be strongly affected by the size and shape of the source at a given total heat release rate.

The effect of radiation heat from the hot layer to the compartment floor represented by temperatures measured at locations of Trees 1, 5, 7 and 9 is represented in Table I. High temperature recorded at Tree 1 position indicated significant radiation heat at the floor level. Owing to the containment of hot combustion products and soot concentrations trapped in the hot layer near the end wall region, strong radiation emissions were encouraged. On the contrary, as dissipation of the hot layer was allowed to migrate into the adjoining room, dissolution of the hot layer with the cold entraining air was promoted thereby reducing the hot layer radiation intensity causing the drop in temperatures at the floor level. It is clearly seen that that simulation considering only gaseous radiation consistently over-predicted the radiation feedback from the hot layer to the floor level at all locations.

The velocity distributions in the vertical plane through the doorway and open end are represented in Figure 5(a) and (b), respectively. Comparison with experimental data was not made available due to instrumental failure of the bi-directional probes in recording the velocity data during the experiments. Nevertheless, as depicted in Figure 5, application of the various models gave very similar velocity profiles. The predicted velocities appeared not to be strongly sensitive to the models used in comparison to the large deviations found in the temperature distributions. The neutral layer height, separating the hot and cold layers, can be located at the inflection point of the velocity profile. At the doorway, the neutral height determined through the case considering soot and gaseous radiation, at approximately 1.1 m, was in between the other two model predictions. It is seen that lower predicted neutral height is accompanied by more inflow of ambient air through the doorway. At the open end of the adjoining room, the handling of the fire through combustion yielded a neutral height of approximately 1.85 m, higher than the height predicted by the volumetric heat source case.

Table I.
 Floor level
 temperatures at
 thermocouple trees
 “1”, “5”, “7” and “9”
 locations

	Tree 1 (°C)	Tree 5 (°C)	Tree 7 (°C)	Tree 9 (°C)
Experiment	125.8	77.6	45.3	22.6
Only gaseous radiation	228.6	180.99	108.83	69.33
Soot and gaseous radiation	85.96	72.59	42.7	32.94

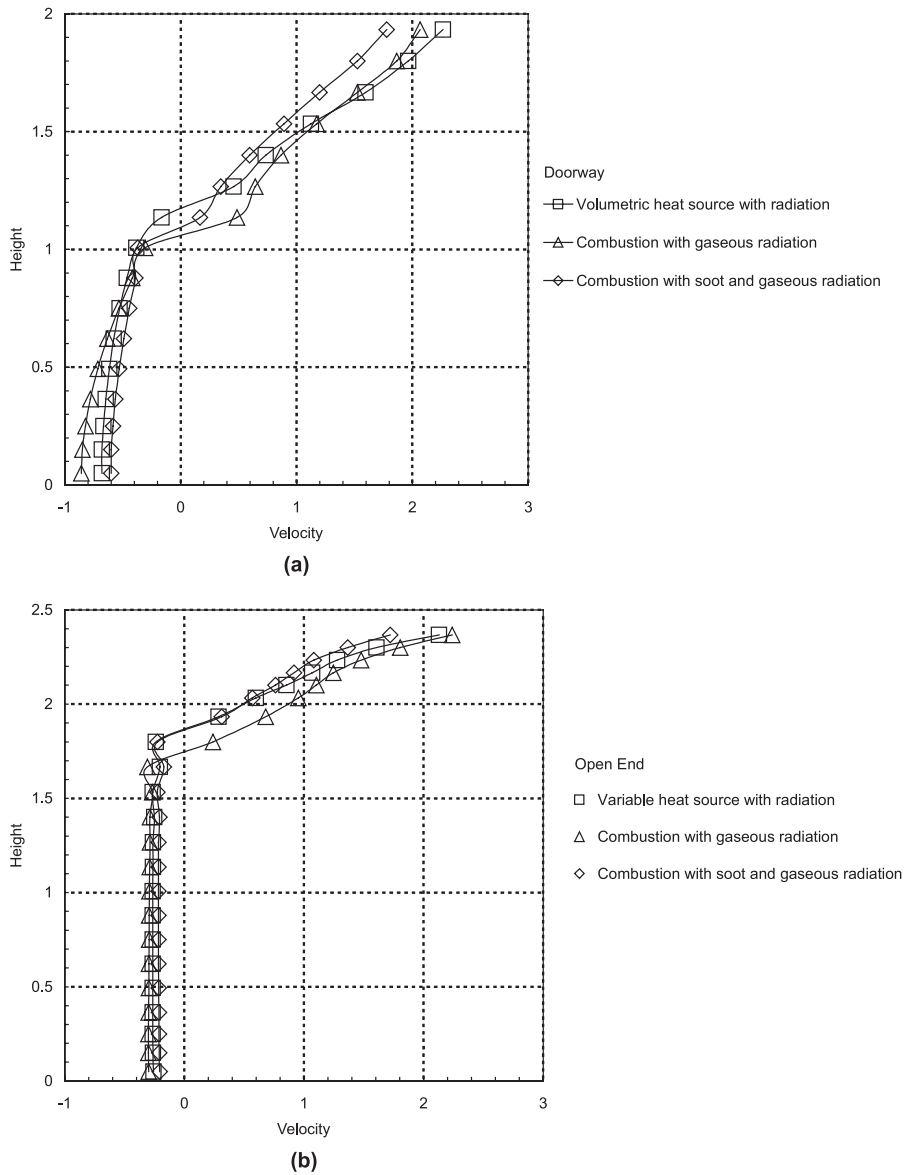


Figure 5.
Velocity profiles: (a)
Doorway and (b) Open
end of the two-
compartment

Distribution of temperature, mass fraction of CO_2 and mass fraction of soot in the vertical plane bisecting the doorway and open end are shown in Figure 6(a)–(c) for the case considering combustion with gaseous and soot radiation. The thermal stratification of the buoyant fire is clearly illustrated by the isotherms in Figure 6(a). In Figure 6(b), the distribution of

CO₂ concentration was significantly diffused within the hot layer below the ceiling of the burn room yielding an average level of around 0.02. Model predictions indicated otherwise for the formation of soot where high soot levels were found trapped within the end wall region. This high soot loading was expected to significantly enhance the absorption of radiation and in turn would significantly lowered the temperatures in the hot layer as predicted in Figure 4(a). On the contrary, the absence of soot consideration would compromise the model predictions with temperatures being over-predicted.

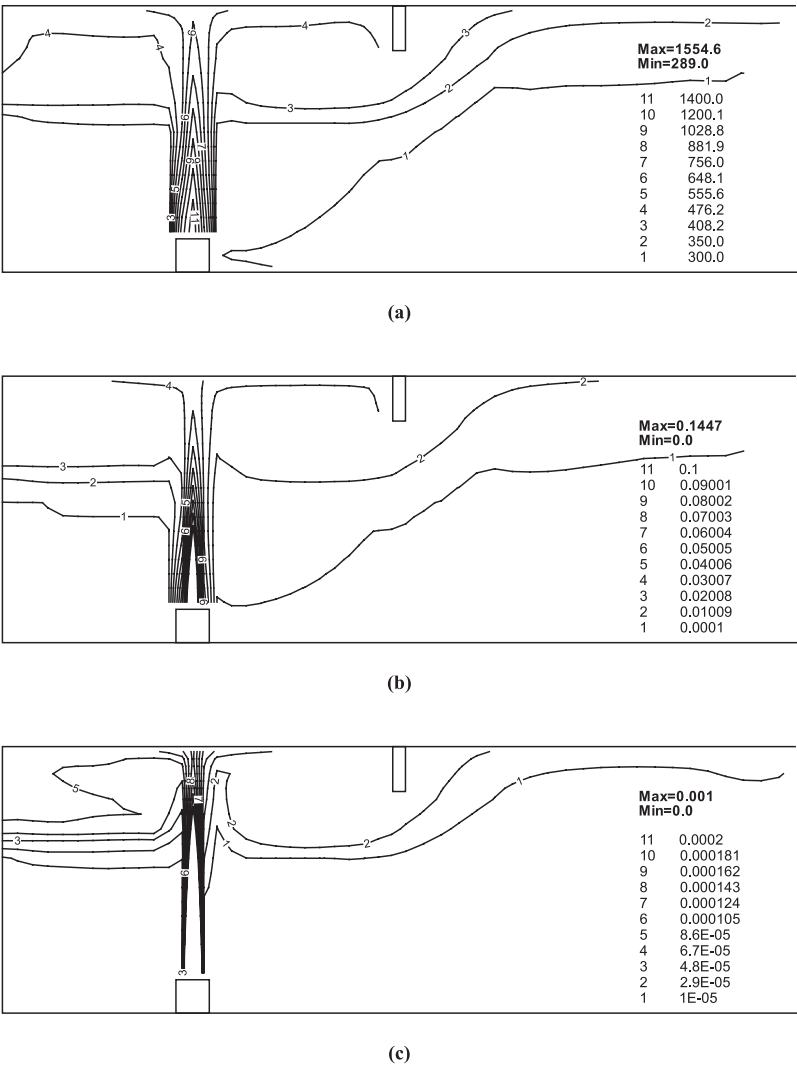


Figure 6.
 Distribution of: (a)
 Temperature, (b) Mass
 fraction of CO₂ and (c)
 Mass fraction of soot on
 a vertical section across
 the centreline of the
 burner, doorway and
 open end of the two-
 compartment

Very low soot concentrations were found in the adjoining room, confirming the inference hypothesised above. Consequently, radiation contribution due to soot would be insignificant. It is noted that an area for further modelling work is to include the effect of turbulent temperature fluctuations on soot generation and the oxidation of soot. The consideration of these effects will only serve to improve the accuracy of the soot model predictions, complementing to its already importance of soot consideration in buoyant fires.

6. Conclusions

This paper presents a CFD modelling of a turbulent buoyant fire in a two-compartment structure. The CFD model comprises solutions to the governing equations for turbulence, combustion, radiation and soot concentration. Validation of the code has been performed against experimental data of Nielsen and Fleischmann (2000). From this study, the following conclusions can be drawn:

- It was apparent that the volumetric heat source approach projected a gross misrepresentation of the temperature distribution above the fire source. The consideration of combustion gave temperature distribution that was consistent with measurements. Although temperatures were adequately predicted in the adjoining room by the volumetric heat source approach, its inaccuracy was left to be desired in the burn room amplifying major limitations in its usage.
- There was good agreement between predicted and measured temperature profiles at various spatial locations within the two-compartment structure especially for the fire model considering combustion with gaseous and soot radiation. The presence of soot was seen to significantly augment the global radiation process in the burn room. Particularly, high soot loading could be found near the end wall of the burn room. The soot pre-exponential constants and activation temperatures used for many methane combustion studies were found to be applicable for the LPG combustion. This investigation clearly demonstrated the need to consider soot generation and its contribution to radiation in enclosure fire simulations.
- Further investigations for the two-compartment fire will involve quantifying the effect of turbulent temperature fluctuations and soot oxidation in the soot model, a parametric study comparing other available soot models and mesh sensitivity.

References

- Beard, A.N. (1997), "Fire models and design", *Fire Safety J.*, Vol. 28, pp. 117-38.
- Drysdale, D. (1986), *An Introduction to Fire Dynamics*, Wiley-Interscience, UK.
- Fuchs, N.A. (1964), *The Mechanics of Aerosols*, Pergamon Press, Oxford.

- Hubbard, G.L. and Tien, C.L. (1978), "Infrared mean absorption coefficients of luminous flames and smoke", *ASME J. Heat Transfer*, Vol. 100, pp. 235-9.
- Jamaluddin, S. and Smith, P.J. (1988), "Predicting radiative transfer in rectangular enclosures using the discrete ordinates method", *Comb. Sci. Tech.*, Vol. 59, pp. 321-40.
- Kent, J.H. and Honnery, D.R. (1990), "A soot formation rate map for a laminar ethylene diffusion flame", *Comb. Flame*, pp. 287-99.
- Lewis, M.J., Moss, M.B. and Rubini, P. (1997), "A. CFD modelling of combustion and heat transfer in compartment fires" *Proc. of 5th Int. Symp. on Fire Safety Sciences*, IAFSS, pp. 463-74.
- Lindstedt, P.R. (1994), "Simplified soot nucleation and surface growth steps for non-premixed flame", in Bockhorn, H., (Eds) *Soot Formation in Combustion: Mechanisms and Models*, Springer-Verlag, Berlin, pp. 417-41.
- Luo, M. and Beck, V. (1996), "A study of non-flashover and flashover fires in a full-scale multi-room building", *Fire Safety J.*, Vol. 26, pp. 191-221.
- Luo, M., He, Y. and Beck, V. (1997), "Application of field model and two-zone model to flashover fires in a full-scale multi-room single level building", *Fire Safety J.*, Vol. 27, pp. 1-25.
- McCaffery (1995), "Flame height", in *The SFPE Handbook of Fire Protection Engineering*, Chapter 1, 2nd ed, Section 2 National Fire Protection Association, Quincy, MA.
- Magnussen, B.F. and Hjertager, B.H. (1976), "On mathematical modelling of turbulent combustion with special emphasis on soot formation and combustion", *Proc. 16th Symp. (Int.) on Combustion*, Combustion Institute, pp. 719-29.
- Markotas, N.C., Malin, M.R. and Cox, G. (1982), "Mathematical modelling for the buoyancy induced smoke flow in enclosures", *Int. J. Heat Mass Transfer*, Vol. 25, pp. 63-75.
- Moss, J.B., Stewart, C.D. and Syed, K.J. (1988), "Flowfield modelling of soot formation at elevated pressure", *Proc. 22nd Symp. (Intern.) on Combustion* Combustion Institute, pp. 413-23.
- Nielsen, C. and Fleischmann, C. (2000), "An analysis of pre-flashover fire experiments with field modelling comparisons", *Fire Engineering Research Report*, ISSN 1173-5996, University of Canterbury, NZ.
- Stone, H.L. (1968), "Iterative solution of implicit approximations of multidimensional partial differential equations", *SIAM J. Numer. Analysis*, Vol. 5, pp. 530-58.
- Steckler, K.D., Quintiere, J.G. and Rinkinen, W.J. (1984), "Flow induced by fire in a compartment", NBSIR 82-2520, National Bureau of Standards, Washington, DC.
- Syed, K.J., Stewart, C.D. and Moss, J.B. (1990), "Modelling soot formation and thermal radiation in buoyant turbulent diffusion flames", *Proc. 23rd Symp. (Intern.) on Combustion*, Combustion Institute, pp. 1533-41.
- Tesner, P.A., Snegiriova, T.D. and Knorre, V.G. (1971), "Kinetics of dispersed carbon formation", *Comb. Flame*, Vol. 17, pp. 253-60.
- Wen, J.X., Huang, K.Y. and Roberts, J. (2001), "The Effect of microscopic and global radiative heat exchange on the field predictions of compartment fires", *Fire Safety J.*, Vol. 36, pp. 205-23.
- Yang, K.T. (1994), "Recent development in field modelling of compartment fires", *JSME Intern. J. Ser. B.*, Vol. 37, pp. 702-17.
- Yeoh, G.H., Yuen, R.K.K. and Chen, D. (2001), "Combustion and heat transfer in compartment fires", paper submitted to *Numer. Heat Transfer*.
- Yuen, R.K.K., Yeoh, G.H. and Chen, D. (2001), "A numerical comparison of combustion and heat transfer in compartment fires", *Proc. 2nd ICHMT Conf. on Advances in Computational Heat Transfer*, pp. 349-56.